JOURNAL
—OF—
THE ROYAL
SOCIETY

Interface

Preliminary comparative study of small amplitude helical and conventional ePTFE arteriovenous shunts in pigs

Colin G Caro, Nick J Cheshire and Nick Watkins

References	**This article cites 13 articles, 3 of which can be accessed free** http://rsif.royalsocietypublishing.org/content/2/3/261.full.html#ref-list-1 Article cited in: **http://rsif.royalsocietypublishing.org/content/2/3/261.full.html#related-urls**
Email alerting service	Receive free email alerts when new articles cite this article - sign up in the box at the top right-hand corner of the article or click **here**

To subscribe to *J. R. Soc. Interface* go to: **http://rsif.royalsocietypublishing.org/subscriptions**

REPORT

Preliminary comparative study of small amplitude helical and conventional ePTFE arteriovenous shunts in pigs

Colin G. Caro[1,†], Nick J. Cheshire[2] and Nick Watkins[1]

[1]*Department of Bioengineering, Imperial College, London SW7 2AZ, UK*
[2]*Regional Vascular Unit, St Mary's Hospital, London W2 1NY, UK*

Intimal hyperplasia (IH), which causes occlusion of arterial bypass grafts and arteriovenous (A-V) shunts, develops preferentially in low wall shear, or stagnation, regions. Arterial geometry is commonly three-dimensional, generating swirling flows, the characteristics of which include in-plane mixing and inhibition of stagnation. Clinical arterial bypass grafts are commonly two-dimensional, favouring extremes of wall shear. We have developed small amplitude helical technology (SwirlGraft) devices and shown them to generate physiological-type swirling flows. Expanded polytetrafluorethylene (ePTFE) grafts, although widely used as A-V shunts for renal dialysis access, are prone to thrombosis and IH. In a small preliminary study in pigs, we have implanted SwirlGraft ePTFE carotid artery-to-jugular vein shunts on one side and conventional ePTFE carotid artery-to-jugular vein shunts contralaterally. There was consistently less thrombosis and IH in the SwirlGraft than conventional shunts. At eight weeks (two animals), the differences were marked, with virtually no disease in the SwirlGraft devices and occlusion of the conventional grafts by thrombosis and IH. The study had limitations, but the lesser pathology in the SwirlGraft devices is likely to have resulted from their geometry and the associated swirling flow. The results could have implications for vascular biology and prolongation of the patency of arterial bypass grafts and A-V shunts.

Keywords: three-dimensional vascular geometry; swirling flow; physiological-type swirling flow; intimal hyperplasia; stagnation regions; swirl induced mixing

†Author for correspondence (c.caro@ic.ac.uk).

1. BACKGROUND

The local flow field in blood vessels influences their biology and development of disease. Both atherosclerosis, which causes heart attack and stroke, and intimal hyperplasia (IH), the principal cause of loss of patency of arterial bypass grafts and arteriovenous dialysis access shunts, develop preferentially in low hydrodynamic wall shear, or stagnation, regions (Caro *et al.* 1971; Sottiurai *et al.* 1989; Bassiouny *et al.* 1992; Giddens *et al.* 1995). Arterial geometry is commonly three-dimensional (Caro *et al.* 1996), and the properties of inertially dominated flows in such geometries include swirling, in-plane mixing, a relatively uniform distribution of wall shear, and inhibition of flow stagnation, separation and instability (Sherwin *et al.* 1997, 2000; Caro *et al.* 1998). Lower limb arterial bypass grafts in patients have been found, however, usually to be essentially two-dimensional (Giordana *et al.* 2005), thus favouring extremes of wall shear, including flow stagnation.

We proposed the use of out-of-plane geometry at arterial bypass grafts, in order to achieve three-dimensionality and physiological-type swirling flow (Sherwin *et al.* 1997, 2000), but judged that the geometry would be difficult to maintain after surgical wound closure (Fontaine *et al.* 2001). We have developed, therefore, small amplitude helical technology (SMAHT) conduits, which we expected to be mechanically robust and have shown in model studies to generate physiological-type swirling flow (Caro 2004). Such conduits could accordingly find application at vascular interventions, including arterial bypass grafts and arteriovenous (A-V) shunts for renal dialysis access.

We describe the properties of SMAHT conduits. We note, in addition, that ePTFE grafts are widely used as A-V shunts in patients requiring renal dialysis, but are prone to early loss of patency, caused by thrombosis and IH (Rotmans *et al.* 2003), a finding which has encouraged the present investigation. We report a small preliminary study in pigs, in which we have compared the performance of SMAHT ePTFE grafts (SwirlGraft devices) with that of conventional ePTFE grafts, both used as A-V shunts. The study was conducted in conformance with the UK Animals Scientific Procedures Act, 1986 and *Guidelines for the Care and Use of Laboratory Animals*, US National Institutes of Health (NIH Publication No. 85-23, revised 1996).

2. METHODS

2.1. Properties of small amplitude helical A-V shunts and model studies

SwirlGraft prostheses were manufactured by thermosetting lengths of 0.6 cm internal diameter (D) ePTFE grafts in mandrels designed to generate the required geometry. Helix pitch and amplitude were defined in terms of D and were approximately $8D$ and $0.4D$, respectively. Two model studies were undertaken to increase understanding of the flow in SMAHT tubes, one involving computational fluid dynamics (CFD) and the other, flow visualization. In both studies, the geometry and time-average flow were similar to
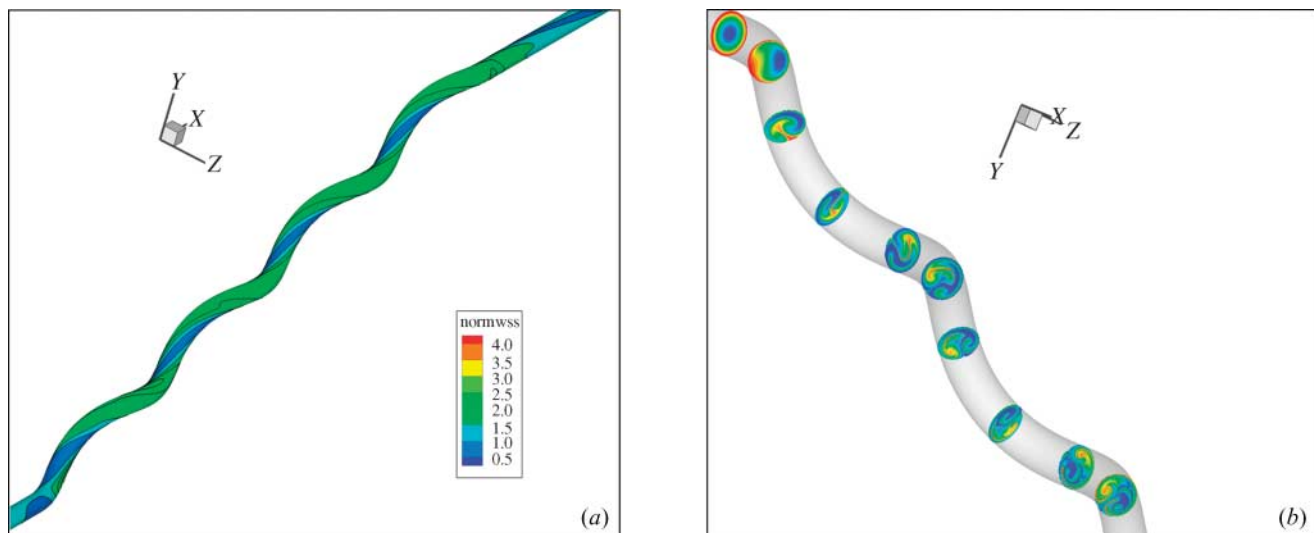
Figure 1. Computational fluid dynamics study of flow in a four-turn helical tube, pitch $10D$, amplitude $0.5D$, Reynolds number 500. (*a*) Contours of wall shear stress normalized relative to that in a Poiseuille flow; flow is from below upward. Rotation of the flow is seen which can continue, although diminishing progressively, in a straight tube downstream. Also seen are ribbons of approximately diametrically opposed relatively low (blue) and relatively high (green) wall shear stress. The flow becomes established in approximately two turns of the helix, with reduction occurring of extremes of wall shear present at the inlet. (*b*) Flow from above downward. Slices normal to the centreline show the position of differently coloured rings of particles as they progress through the tube. There is substantial in-plane mixing within half a turn of the helix. The mixing can continue, although diminishing progressively, in a straight tube downstream (not shown in figure).

those expected to be present in the *in vivo* study. Pulsatility can influence mixing and we have undertaken preliminary investigations of pulsatile flow in non-planar configurations. The present model studies have been confined, however, to steady flow, consistent with the reported relatively low pulsatility of renal dialysis access shunt flow.

The CFD study involved a four-turn helical tube with pitch and amplitude approximately $10D$ and $0.5D$, respectively, and Reynolds number 500 (a value calculated from measurements of flow and vessel diameter made at porcine A-V access grafts; Rotmans *et al.* 2003). As illustrated in figure 1*a*, there was swirling flow, which continued into a straight tube downstream of the helical tube. Consistent with swirling flow in a helical tube, there were ribbons of approximately diametrically opposed relatively low and relatively high wall shear stress. As shown in figure 1*b*, there was, in addition, the development of extensive in-plane mixing, within half a turn of the helix.

The flow visualization study involved the injection of a bolus of ink into water flowing at a Reynolds number of 550, in either a U-tube constructed from conventional tubing, or a U-tube with similar curvature, but constructed from a SMAHT tube (figure 2). In the former case, the indicator dispersed axially and had a long residence time in the inlet tube and at the inner wall of curvature of the U-bend, whereas in the SMAHT U-tube, axial dispersion was markedly less, as was retention of the indicator in the inlet tube and at the inner wall of curvature of the U-bend.

2.2. Animal study

The pigs weighed at least 40 kg. Under general anaesthesia (xylazine 1 mg kg^{-1} i/m, ketamine 5 mg

kg^{-1} i/m, oxygen and nitrous oxide ($2:1$) and halothane (2%)) a 14 cm long 0.6 cm internal diameter SwirlGraft was implanted in each animal in end-to-side loop conformation connecting the left common carotid artery and left jugular vein; a 14 cm long conventional 0.6 cm internal diameter ePTFE graft was similarly implanted contralaterally. In view of the liability of ePTFE grafts in pigs to thrombosis (Rotmans *et al.* 2003), the animals received daily, starting 1 day preoperatively and continuing until termination, 75 mg acetylsalicylic acid and 225 mg Clopidogrel (Sanofi-Synthelabo, Paris, France).

It was planned to sacrifice two animals at each of 2, 4 and 8 weeks after graft implantation, when the grafts would be explanted and subjected to histopathologic study. However, two animals died within hours of graft implantation, one from generalized bleeding and hyperthermia and the other from heart failure, necessitating their exclusion from the study. One further animal was added to the study.

At termination, the animals were anaesthetized, the grafts were exposed and heparin (100 iu kg^{-1}) was administered intravenously before manipulation of the vessels. Because extensive post-implantation fibrosis made dissection difficult, flow monitoring (Dopplex II, Huntleigh Healthcare) had to be confined to the common carotid artery proximal to the artery–graft junction (anastomosis). The artery was cannulated and the graft and associated vessels were flushed with saline. The animal was then euthanized, the grafts were pressure-perfused with formalin, taking care to prevent reflux of blood, and the grafts and associated vessels were excised en bloc and immersed in formalin.

The formalin-fixed vessels were cut into 5 mm blocks, locally perpendicular to the graft/vessel axis. These were assembled serially and photographed before
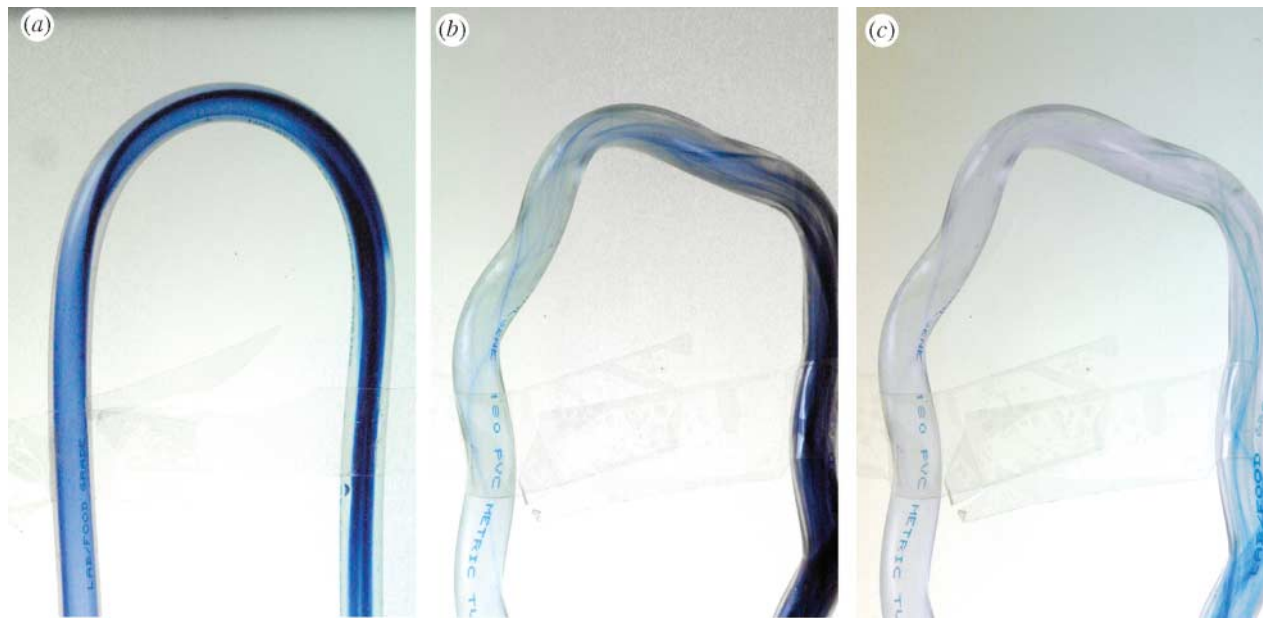
Figure 2. Bolus injection of 0.5 ml ink into water flowing (Reynolds number 550) in 0.8 cm internal diameter (D) pvc U-tubes, tube radius/radius of curvature approximately 0.1. (a) Conventional tube; (b), (c) SMAHT tube, amplitude ratio and pitch approximately $0.5D$ and $6D$, respectively. In (a), axial dispersion is seen of the indicator, which has a long residence time in the inlet tube (left) and at the inner wall of curvature of the U-bend. In (b) and (c), sequential images of flow in SMAHT tube, axial dispersion of the indicator is reduced, as its retention in the inlet tube (left) and at the inner wall of curvature of the U-bend.

embedding in paraffin. Sections were prepared of the vessels proximal and distal to the artery–graft junction, of the graft, and of the vessels proximal and distal to the graft–vein junction. The sections were EvG stained for general morphology and measurement of intimal and medial thickness. They were stained with haematoxylin and eosin to distinguish IH from organized thrombus.

3. RESULTS

Because of the early losses, only five animals could undergo graft explantation at the planned times. One two-week animal, PC2, had a large, tense, lymphatic fluid-filled swelling (seroma) in the upper thorax, which was compressing the trachea and was presumed responsible for the observed bilateral thrombosis of the grafts. This animal's results were excluded from the study. The development of seromas is a recognized complication of graft implantation; there were no seromas in any of the other animals.

The other two week animal, PC3, had a small amount of thrombus in four of the conventional graft 5 mm blocks, whereas the SwirlGraft was virtually free of thrombus. There was a small amount of IH in both the SwirlGraft and the conventional graft, but more in the latter. Only one animal, PC5, was sacrificed at four weeks; there was a small amount of thrombus in four of the conventional graft 5 mm blocks, whereas there was a small amount in one SwirlGraft block and a very small amount in another.

There were marked differences between the conventional grafts and the SwirlGraft grafts in the two animals sacrificed at eight weeks (PC4 and PC7). In PC4 (figure 3), the conventional graft was occluded by thrombus and clot along approximately its distal

half. The occlusion continued into the graft–vein anastomosis and the vein distal to the anastomosis was occluded by IH and fibrosis. The SwirlGraft was patent throughout its length and there were only approximately diametrically opposed ribbons of pathology. The graft–vein anastomosis and vein distal to the anastomosis were patent. There was some IH at the graft–vein anastomosis and in the vein distal to the anastomosis, but because of dilatation of the vessel, there was no reduction of the cross-sectional area.

In PC7 (figure 4), the findings were similar. In the conventional graft there was a small amount of IH distal to the artery–graft junction. Progressing distally, there was extensive thrombosis with some mineralization implying relatively long-standing pathology, culminating in occlusion of the graft. The graft–vein anastomosis and vein distal to the anastomosis were totally occluded. The SwirlGraft was patent throughout its length, with only minimal IH. The IH was usually present as two approximately diametrically opposed seemingly helical ribbons, which were histologically different and occupied only approximately 5% of the graft cross-section. The graft–vein anastomosis and vein distal to the anastomosis were patent. There was some IH in the vein distal to the anastomosis, but because of dilatation of the vessel there was no reduction of cross-sectional area.

4. DISCUSSION AND CONCLUSIONS

The objectives of this preliminary study were to assess the liability of conventional and SwirlGraft ePTFE A-V shunts to develop pathology and the surgical characteristics of the grafts. The study had several limitations. Among these were the small number of animals, the implantation of the SwirlGraft devices in

Figure 3. Five mm blocks from animal PC4, cut perpendicular to graft/vessel axis and assembled serially: (*a*) conventional grafts, (*b*) SwirlGraft grafts. In both grafts, the artery–graft anastomosis is above. The conventional graft is progressively thrombosed, proceeding distally from the artery–graft anastomosis and culminating in its occlusion. In addition, the graft–vein anastomosis is occluded, and the vein distal to the anastomosis is collapsed and fibrosed. In contrast, the SwirlGraft grafts are patent throughout their length and the graft and graft–vein anastomoses are almost free of thrombus. There is some IH in the veins distal to the graft–vein anastomoses, but the vessels are patent and because of dilatation there is no reduction of cross-sectional area. Visible in SwirlGraft sections are approximately diametrically opposed seemingly helically distributed ribbons of pathology.

each animal exclusively between the left common carotid artery and left jugular vein, the derivation of the conventional and SwirlGrafts (though composition-ally and dimensionally similar) from different manu-facturers, the inadequacy of graft imaging and the absence of measurement of graft flow. In relation to the last, it seems unlikely from model studies that the flow rates were grossly different in any animal in the conventional and SwirlGraft grafts.

Despite these limitations, the consistently lesser pathology in the SwirlGraft A-V shunts and outflow vessels than in the conventional A-V shunts and outflow vessels (the difference being slight at two and four weeks, when there was little disease overall, but marked at eight weeks) would seem to merit reporting. It would seem indicated, furthermore, to consider briefly underlying mechanisms and the significance of the findings.

It seems improbable that the derivation of the ePTFE grafts from different manufacturers could *per se* account for the observed differences in pathology between the conventional and SwirlGraft devices. The ePTFE grafts supplied by both manufacturers are widely used in clinical practice and both manufacturers supply clinically widely used ePTFE grafts that have

been subjected to additional thermosetting to alter their geometry, for example, to produce tapering.

Instead, it appears likely from the preferred occur-rence of IH in low wall shear regions and the predicted differences in the flow between the conventional and SwirlGraft devices, that fluid mechanical factors played an important role. As noted, model studies lead to the expectation of swirling flow, in-plane mixing, relative uniformity of wall shear, and inhibition of flow stagnation, separation and instability in the SwirlGraft devices and graft–vein junctions. Such flow could, by virtue of mixing, enhance fluid/wall mass transport in non-curved conduits. Moreover, as implied by the results illustrated in figure 2, it could enhance fluid/wall mass transport and render the spatial distribution of wall shear relatively uniform in curved conduits, and potentially at anastomoses. Furthermore, the flow could, via effects of fluid mechanical forces, including wall shear stress, profoundly influence vessel wall biology (Davies 1995; Gimbrone 1999; Garcia-Cardena *et al.* 2001; Tarbell 2003).

The CFD studies (figure 1) predict the presence of approximately diametrically opposed helical ribbons of relatively high and relatively low wall shear along helical conduits, under the expected conditions. The
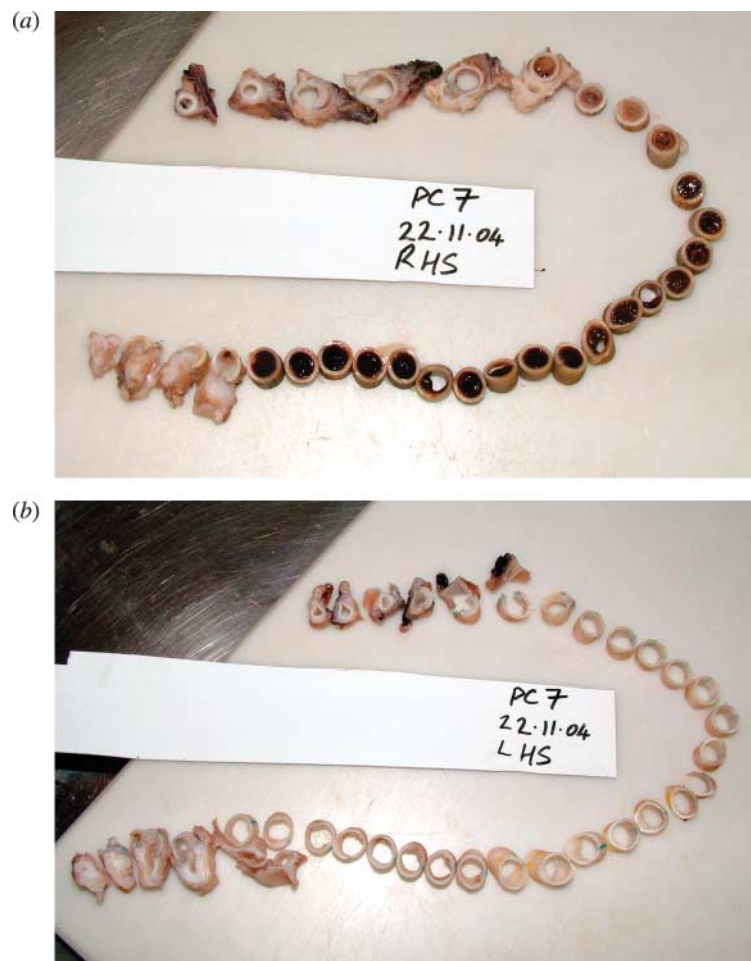
Figure 4. Five mm blocks from animal PC7, cut perpendicular to graft/vessel axis and assembled serially: (*a*) conventional grafts, (*b*) SwirlGraft grafts. In both grafts, the artery–graft anastomosis is above. The conventional graft is progressively thrombosed, proceeding distally from the artery–graft anastomosis and culminating in its occlusion. In addition, the graft–vein anastomosis is occluded, and the vein distal to the anastomosis is collapsed and fibrosed. In contrast, the SwirlGraft grafts are patent throughout their length and the graft and graft–vein anastomoses are almost free of thrombus. There is some IH in the veins distal to the graft–vein anastomoses, but the vessels are patent and because of dilatation there is no reduction of cross-sectional area. Visible in SwirlGraft sections are approximately diametrically opposed seemingly helically distributed ribbons of pathology.

presence of two seemingly helical ribbons of pathology along the grafts is therefore consistent with the fluid mechanics significantly influencing the biological/pathological processes.

No greater surgical difficulty was experienced in implanting the SwirlGraft devices than the conventional grafts and the SwirlGraft geometry appeared to be maintained *in situ*. Contingent on confirmation of these findings, there may be general implications for vascular biology and implications for prolongation of the patency of vascular interventions, including arterial bypass grafts and arteriovenous shunts for renal dialysis.

REFERENCES

Bassiouny, H. S., White, S., Glagov, S., Choi, E., Giddens, D. P. & Zarins, C. K. 1992 Anastomotic intimal hyperplasia: mechanical injury or flow induced. *J. Vasc. Surg.* **15**, 708–717.

Caro, C. G., Fitz-Gerald, J. M. & Schroter, R. C. 1971 Atheroma and arterial wall shear. Observation, correlation and proposal of a shear dependent mass transfer mechanism for atherogenesis. *Proc. R. Soc. B* **177**, 109–159.

Caro, C. G., Doorly, D. J., Tarnawski, M., Scott, K. T., Long, Q. & Dumoulin, C. L. 1996 Non-planar curvature and branching of arteries and non-planar-type flow. *Proc. R. Soc. A* **452**, 185–197.

Caro, C. G., Watkins, N., Doorly, D. J., Sherwin, S. J. & Peiró, J. 1998 Influence of non-planar geometry on flow separation. *J. Physiol.* **513**, 2.

Caro, C. G. 2004 Flow in arteries and large airways. Invited Lecture, Euromech 456, RWTH Aachen, October 4. (available on video).

Davies, P. F. 1995 Flow-mediated endothelial mechanotransduction. *Physiol. Rev.* **75**, 519–560.

Fontaine, E. J., Caro, C. G., Anderson, J. R. & Watkins, N. 2001 Aorto-coronary vein graft geometry: a preliminary study breaking symmetry in haemodynamics. In *British Heart Foundation Workshop, Imperial College, April 23–24, 2001* p. 50.

Garcia-Cardena, G., Comander, J. I., Blackman, B. R., Anderson, K. R. & Gimbrone, M. A. 2001 Mechanosensitive endothelial gene expression profiles: scripts for the role of hemodynamics in atherogenesis. *Ann. NY Acad. Sci.* **947**, 1–6.

Giddens, D. P., *et al.* 1995 Fluid dynamics of end-to-side vascular grafts. In *Biological flows* (ed. M. Jaffrin & C. G. Caro). World Congress of Biomechanics Series, vol. 1. New York: Plenum Publishing Corporation.

Gimbrone, M. A. 1999 Vascular endothelium, hemodynamic forces and atherogenesis. *Am. J. Pathol.* **155**, 1–5.

Giordana, S., *et al.* 2005 Automated classification of peripheral distal by-pass geometries reconstructed from medical data. *J. Biomech.* **38**, 47–62.

Rotmans, J. L., Velema, E., Verhagen, H. J. M., Blankensteijn, J. D., Kastekin, J. J. P., Kleijn, D. P. V., Pasterkamp, G. & Stroes, E. S. G. 2003 Rapid arteriovenous graft failure due to intimal hyperplasia: a porcine, bilateral, carotid arteriovenous graft model. *J. Surg. Res.* **113**, 161–171.

Sherwin, S. J., Shah, O., Doorly, D. J., McLean, M., Watkins, N., Caro, C. G., Peiró, J., Tarnawski, M. & Dumoulin, C. L. 1997 Visualisation and computational study of flow at model planar and non-planar end-to-side arterial bypass grafts. *J. Physiol.* **504**, 44.

Sherwin, S. J., Shah, O., Doorly, D. J., Peiró, J., Papaharilaou, Y., Watkins, N., Caro, C. G. & Dumoulin, C. L. 2000 The influence of out-of-plane geometry on the flow within a distal end-to-side anastomosis. *ASME J. Biomech.* **122**, 1–10.

Sottiurai, V. S., Yao, J. S. T., Batson, R. C., Sue, S. L., Jones, R. & Nakamura, Y. A. 1989 Distal anastomotic intimal hyperplasia: histopathologic character and biogenesis. *Ann. Vasc. Surg.* **3**, 26–33.

Tarbell, J. M. 2003 Mass transport in arteries and the localization of atherosclerosis. *Annu. Rev. Bioeng.* **5**, 79–118.